J Mater Sci: Mater Med (2014) 25:229–237
DOI 10.1007/s10856-013-5056-5

Dielectric study of the adhesion of mesenchymal stem cells from human umbilical cord on a sugarcane biopolymer

A. S. Fragoso · M. B. Silva · C. P. de Melo · J. L. A. Aguiar · C. G. Rodrigues · P. L. de Medeiros · J. F. Branco Junior · C. A. S. Andrade · M. D. L. Oliveira

Received: 20 March 2013 / Accepted: 16 September 2013 / Published online: 27 September 2013

Abstract It is of current interest the identification of appropriate matrices for growing mesenchymal stem cells (MSC). These cells are able not only to regenerate themselves but also to differentiate into other type of functional cells, and so they have been extensively used in tissue engineering. In this work, we have evaluated the use of electric impedance spectroscopy (EIS) to follow the adhesion of MSC from Wharton's jelly of the human umbilical cord (hWJMSC) on sugarcane biopolymers (SCB). Impedance spectra of the systems were obtained in the frequency range of 10^2–10^5 Hz. An EIS investigation showed that when deposited on a metallic electrode SCB films prevent the passage of electrons between the solution and the metallic interface. The impedance spectra of hWJMSCs adhered on SCB revealed that there is a significant increase in the magnitude of the impedance when compared to that of pure SCB. The corresponding resistance (real part of the impedance) was even higher for the SCB–hWJMSC system than for SCB without cells on their surface, in an indication of an increased blockage to the electron transfers. The resistance charge transfer is extracted by curve-fitting the impedance spectra to an equivalent circuit model. Also, a shift of the phase angle to higher frequencies was obtained for SCB–hWJMSC system as a result from hWJMSC adhesion. Our study demonstrates that EIS is an appropriate method to evaluate the adhesion of MSC. SCB can be considered as a promising biomaterial for tissue engineering.

A. S. Fragoso · M. D. L. Oliveira
Programa de Pós-Graduação em Ciências Biológicas, Universidade Federal de Pernambuco, Recife, PE 50670-901, Brazil

M. B. Silva · C. G. Rodrigues · J. F. Branco Junior
Departamento de Biofísica e Radiobiologia, Universidade Federal de Pernambuco, Recife, PE 50670-901, Brazil

C. P. de Melo
Departamento de Física, Universidade Federal Pernambuco, Recife, PE 50670-901, Brazil

J. L. A. Aguiar
Departamento de Cirurgia, Universidade Federal de Pernambuco, Recife, PE 50670-901, Brazil

P. L. de Medeiros
Departamento de Histologia e Embriologia, Universidade Federal de Pernambuco, Recife, PE 50670-901, Brazil

C. A. S. Andrade · M. D. L. Oliveira (✉)
Departamento de Bioquímica, Universidade Federal de Pernambuco, Recife, PE 50670-901, Brazil
e-mail: m_danielly@yahoo.com.br

1 Introduction

Desirable properties for polymers useful for tissue engineering applications include high conductivity, reversible oxidation, redox stability, biocompatibility and low hydrophobicity [1]. A common goal in tissue engineering is to attain the ability to tailor specific cell-support interactions and thereby gain control over cell behavior. An ideal biomaterial would thus combine properties as biocompatibility, biodegradability and diminished cytotoxicity. These properties are normally found in materials formed by complex carbohydrates similar to extracellular matrix [2].

Sugarcane biopolymer (SCB) is a polysaccharide with high elasticity, resistance to traction and good mechanical flexibility. SCB is a natural exopolysaccharide obtained through the action of bacteria of the species *Zoogloea* sp., with culturing in sugarcane molasses, and its chemical structure is composed of different monosaccharides as follow: glucose 87.57 %, xylose 8.58 %, ribose 1.68 %,

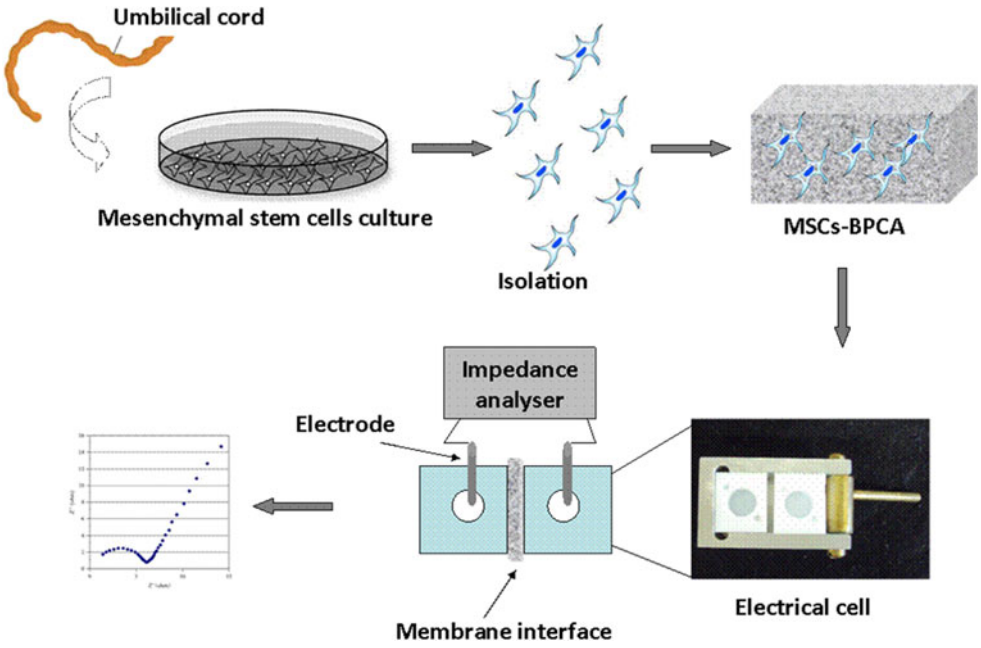

Fig. 1 Schematic representation of the hWJMSC adhesion and of the measurement apparatus

glucuronic acid 0.83 %, mannose 0.82 %, arabinose 0.37 %, galactose 0.13 %, rhamnose 0.01 % and fucose 0.01 % [3].

It is worth to note that SCB has been used to induce cellular adhesion and proliferation in different animal models and various body tissues, with the purpose of repair, replacement or support [3–6]. SCB is a very competitive polymer compared to other similar materials due to its low toxicity, high osteoconductivity, low production cost, biocompatibility and capability of integration with different living tissues. Recently, SCB has also been used to repair osteochondral defects in femurs of rabbits, when it was shown that it leads to a reduction of the healing time by significantly enhancing the proliferation of osteochondral cells [4]. In addition, SCB has been used in arterial prosthesis, in the reconstruction of tympanic membrane and of the urethra and as a graft in rat bladders, always with good integration [5]. In fact, SCB showed an excellent biocompatibility for use as suture material [5]. Thus, these findings suggest the applicability of SCB as a convenient matrix to cellular adhesion and scaffolds to tissues engineering.

In recent years, mesenchymal stem cells (MSC) from Wharton's jelly of the human umbilical cord (hWJMSC) have been extensively studied since they are a potential source of cells for therapeutic strategies, such as tissue engineering [7, 8]. In addition, hWJMSC are capable of not only to regenerate themselves but also to differentiate into several other type of functional cells, such as muscle and adipose cells [7, 8]. Also, hWJMSC has been used with success in medicine when evaluating animal models for regeneration of bone, cardiomyocytes and neurons [9–11].

Currently, electrical impedance spectroscopy (EIS) is one of the most powerful and convenient tools to evaluate interfacial phenomena and interactions between biomolecules. As a sensitive and effective method to probe the interfacial properties of modified electrodes, this technique has found widespread applications in various fields [12, 13]. By measuring the frequency dependence of the electrical properties of living cells and tissues EIS can provide physiological and morphological information [14, 15] and in this manner it has been also employed to assess the metabolism of living cells in vitro [16]. Furthermore, EIS has been used for monitoring neural cell behavior on electroactive polymers for tissue repair strategies [17] and in the dynamic monitoring of cell-surface glycan expression to evaluate structural variations in cellular physiology [18].

In the present work we have used EIS to assess the characteristics of SCB films both in pristine form and also when used as matrices for the deposition of hWJMSC. To the best of our knowledge, this is the first report of a dielectric investigation on the nature of the SCB–hWJMSC interaction. In this study, we evaluate this interaction by disposing SCB and hWJMSC in a homemade cell composed by two small (5 mL) wells separated by a Teflon barrier connected through a small diameter ($\phi = 1$ mm) orifice (Fig. 1). Our main objective was the characterization and investigation of hWJMSC to SCB polymer surface by using EIS, atomic force microscopy (AFM) and Fourier transform infrared spectroscopy (FTIR). The EIS was utilized to quantify the electron transfer resistance (R_{et}) of SCB films of different thickness and under varying applied potentials, before and after the adhesion of hWJMSC on the SCB surface. The impedance values of the adhered hWJMSC were measured and calculated. As a result, we have been able to establish

that indeed EIS is a convenient technique to investigate the process of adhesion of hWJMSC to biopolymer surfaces.

2 Experimental procedure

2.1 Materials

Dulbecco's minimum essential medium (DMEM, with 4.5 % g/L D-glucose), fetal bovine serum (FBS) and Ham's F12 Nutrient Mixture were all purchased from Life Technologies (USA). All chemicals and solvents were of analytical-grade and used as received, without further purification. High-purity water was obtained after a Milli-Q plus (Billerica, USA) treatment.

2.2 SCB obtention

SCB was obtained from the bacteria *Zoogloea* sp. using medium containing glucose, yeast extract, peptone and agar, as indicated by Carvalho Junior et al. [5]. Raw material consisted of sugar cane molasses adjusted to a 15 % brix (pH 5.0). The culture was inoculated in erlenmeyers at 30 °C for up to 7 days. The resulting material was then dried in incubator with air circulation and sterilized in autoclave at 120 °C.

2.3 Infrared spectroscopy measurements

FTIR of the SCB layers was obtained by use of a Bruker FTIR spectrometer (Bruker Optics Inc., USA) that allowed us to record spectra between 4,000 and 700 cm^{-1}. Resolution was fixed at 4 cm^{-1} and 60 scans were performed to acquire each spectrum.

2.4 Morphological analysis

AFM measurements were made using a Witex microscope (Molecular Imaging, USA). Cantilevers with a Cr–Au tip (NSC18, MikroMasch, $F_0 = 90$ kHz, nominal spring constant = 5.5 N m^{-1}) were used in tapping mode AFM [19]. AFM experiments were performed in air at room temperature (~25 °C), and 5 × 5 μm^2 areas of the samples were scanned with a resolution of 512 × 512 pixels. On each sample, AFM images were obtained from at least two macroscopically separated areas, to eliminate artifacts. Cell adhesion and morphology were evaluated with a scanning electron microscopy (SEM) (JSM 5900, JEOL Instruments, Japan) at an acceleration voltage of 5 kV and at a working distance of 5 μm.

2.5 Cell culture on SCB surface

SCB film was sterilized with a (7:1, v/v) solution of ethanol:water and then exposed to ultraviolet light. Subsequently, MSC from hWJMSC (cellular density of 1.6×10^5 cells/cm^2) cultured in DMEM supplemented with 15 % FBS and 20 % F-12 were added to the SCB surface, and then incubated at 37 °C in 5 % CO_2 for 24 h to allow the investigation of the cell adhesion process. Viable cells were counted using a common hemocytometer. After the incubation, the hWJMSC-modified SCB film was washed with phosphate buffer saline to remove non-adherent cells, detached from the culture plates and then placed in the homemade cell containing stainless steel electrodes (Fig. 1). EIS was used to collect the Z′ values as a function of the time required to assess the adhesion process of hWJMSC on the SCB surface.

2.6 AC impedance recording and analysis

AC electrical impedance was used to probe the changes in the electrical behavior of the cells that accompany the induced differentiation. Data acquisition of the dielectric response was performed using a SI 1260 gain/phase impedance analyzer (Solartron Instruments, UK) for determining the real (Z′) and imaginary (Z″) parts of the impedance. The electrical impedance spectra were recorded in the 10^2–10^5 Hz frequency range. The amplitude of applied wave potential was 10 mV and the applied potential varied from 0.2 to 1.0 V. All measurements were performed in triplicate.

3 Results and discussion

3.1 Infrared spectroscopy analysis

In order to analyze the chemical nature of the carbohydrate polymer films, we collected the FTIR spectra from the SCB films. These corresponding spectra confirmed the presence of the main SCB characteristic vibration bands. The FTIR spectrum shown in Fig. 2 corresponds to the structure of a typical polysaccharide with the characteristic band between 1,200 and 900 cm^{-1} that can be attributed to the carbohydrate C–O–C bond, and this confirms the presence of links between the carbohydrate units forming the biopolymer. We also observed the OH stretching band between 3,600 and 3,000 cm^{-1}. In addition, the FTIR spectrum contains an angular deformation at 1,639 cm^{-1} that confirms the presence of monosaccharides. The asymmetric stretching of the CH_2 groups is observed from 2,900 to 2,950 cm^{-1} [20].

3.2 Optical characterization

We performed an AFM analysis to elucidate the variation of the topography and the morphology of the SCB biopolymer. A representative image of a 5 × 5 μm area of the

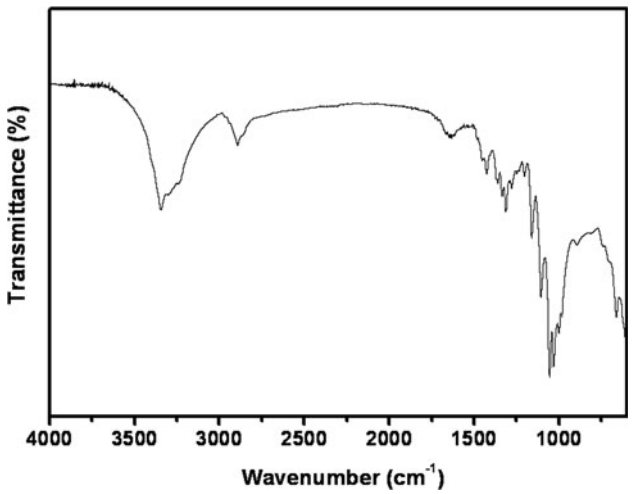

Fig. 2 Infrared spectra of the sugar cane biopolymer film

SCB film is shown in Fig. 3a. The AFM 3D topographical view (Fig. 3a) showed that SCB consists of a large number of quite evenly distributed hill-valley-structure surfaces, with some regular pores present in the nanoscale topography. In Fig. 3b, c we show the 2D height and profile images, respectively. The analysis of Fig. 3b, c can provide quantitative information about the polysaccharide surface and the diameter of the aggregates based on the vertical and horizontal distances on the surface, respectively. A section analysis can be performed by drawing a cross-sectional line over the image. One can note that the SCB films present an irregular morphology with very characteristic features, such as the presence of fibers and a granular morphology that differ in height by $\sim$190 nm.

The morphology of hWJMSC deposited on the surface of a SCB film was assessed using a SEM to evaluate the shape and adherence of the cell. SEM micrographs of hWJMSC on SCB surface are presented in Fig. 4. The hWJMSC adhered to the surface of the SCB that, as previously discussed, presents an evenly distributed hill-valley-structure (Fig. 4a), revealing satisfactory cell adhesion and undifferentiated cell characteristics (Fig. 4b). It is known that tissue-derived cells are anchorage dependent and must adhere to a solid surface to grow and proliferate and that this step precedes further events such as cell migration and differentiation [21].

3.3 Dielectric evaluation of the SCB film as a matrix to culture cells

EIS has previously been shown to be a powerful tool to evaluate the dielectric response associated to cell adhesion on polymer surfaces [22]. AC impedance was recorded at 10^2–10^5 Hz with an applied polarization potential varying from 0.2 to 1.0 V.

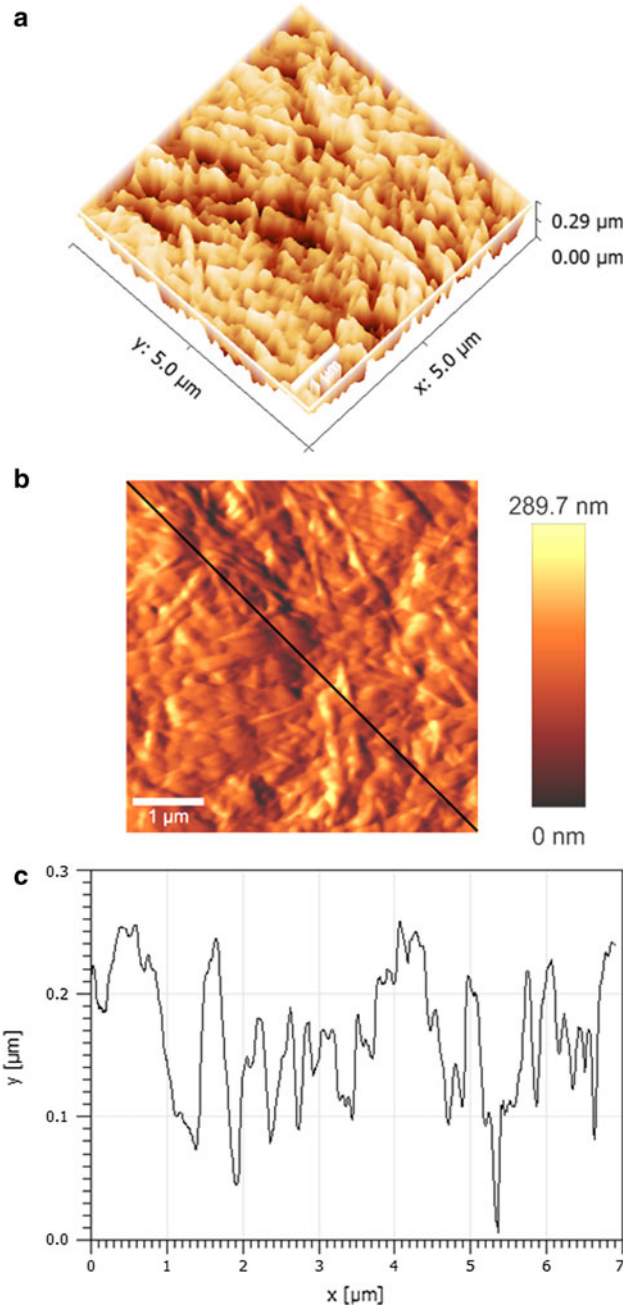

Fig. 3 3D (**a**) and 2D (**b**) AFM topographic images (5 × 5 μm^2) of the SCB. A section analysis along the *black line* in (**b**) shows that the step height (**c**) between higher and lower levels is $\sim$259 nm

The measurements were carried out by using EIS to evaluate the influence of cell adhesion on the polymer matrix. Therefore, SCB films of different thicknesses were used as follows: SCB1 (19 µm), SCB2 (23 µm) and SCB3 (31 µm). In addition, for each one of these SCB films the EIS spectra were evaluated under different potentials (0.2, 0.4, 0.6, 0.8 and 1.0 V), as shown in Fig. 5. As expected, the film SCB1 presented lower R_{et} values at different potentials as compared to the values obtained for SCB2 and

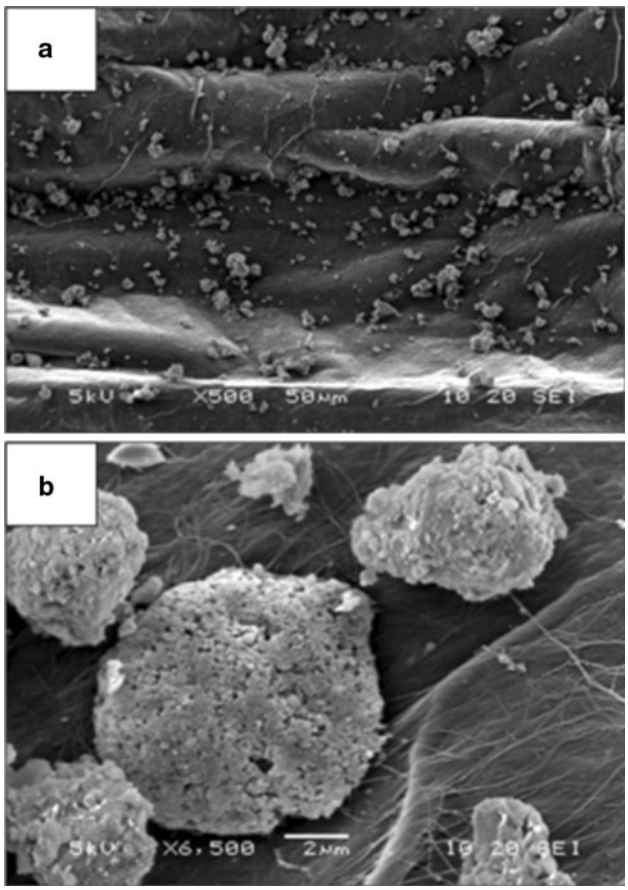

Fig. 4 Cell adhesion and morphology by SEM of hWJMSC–SCB system (**a**). Higher magnification of the hWJMSC–SCB (**b**)

SCB3, confirming that the electron transfer blockage is related to the thickness of the biopolymer films.

An EIS analysis of the SCB without stem cells demonstrated lower values of Ret. As expected, the dielectric characteristics of the system are altered when more molecules and/or materials are adsorbed on the electrode surface, a fact that is reflected as an increase of the electron resistance. In our case, after adhesion of hWJMSC on the biopolymer surface, an additional blockage of the electron transfer between work electrode and the solution is observed. Therefore, in this work we demonstrated the use of EIS as an alternative technique to evaluate the adhesion of MSC on biopolymer surface.

In Fig. 5 we show the Faradaic impedance spectra before and after the polysaccharide surface modification resulting from the MSC incubation. The cell adhesion resulted in a significant increase of the electron transfer resistance. Accordingly, estimated R_{et} values for the stem cells-modified SCB surfaces were higher by about 98.08 MΩ, as compared to those of pure SCB films. After introducing the hWJMSC on the SCB surface, the values of R_{et} increased from 24.0 to 98.08 MΩ, in an indication that the cells adhere to the biopolymer surface. Thus, the

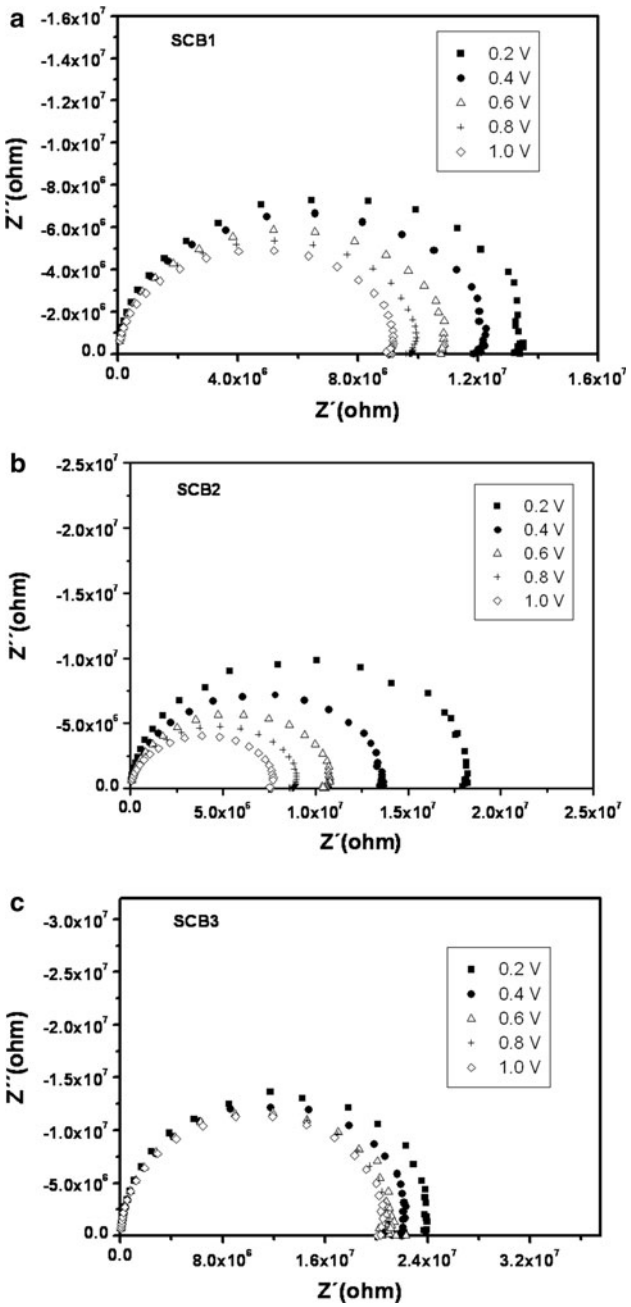

Fig. 5 Nyquist plots of the SCB at different applied potentials: SCB1 (**a**), SCB2 (**b**) and SCB3 (**c**)

adhesion of hWJMSC lead to a decrease of the active surface area and to an increase of the barrier effect against the electron transfer between the biofilm and the electrode surface. The changes in the impedance response of the SCB film can be attributed to the adhesion of the stem cells to the polymer network present in the SCB layer.

In the case of stem cells, important cellular processes (such as growth, morphology and differentiation) are controlled by extracellular signals received at the cell's surface [23]. In general, some external stimuli are received in

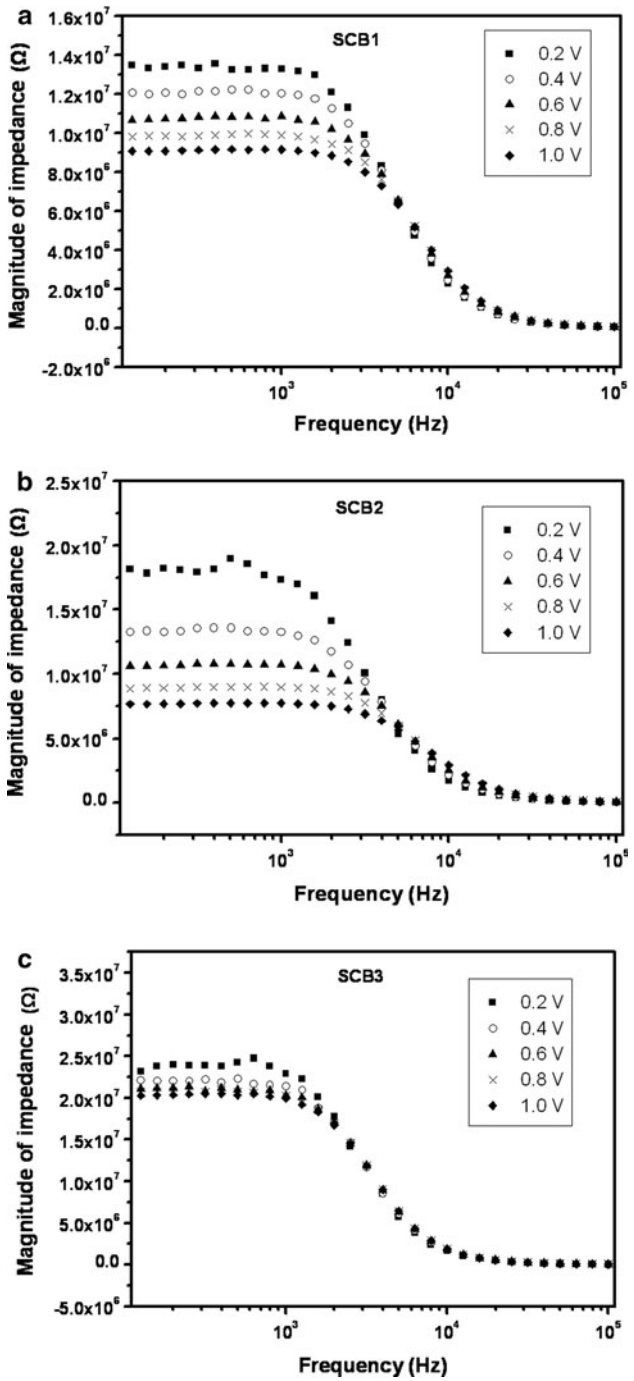

Fig. 6 Bode plots of the SCB at different applied potentials: SCB1 (**a**), SCB2 (**b**) and SCB3 (**c**)

soluble form in extracellular fluids; however, other signals are part of a neighboring cell surface. In this way, a complex cell surface code may direct intercellular interactions as diverse as the binding of pathogens to their target tissues [24] and stem cells adhesion to polymers [25]. Guo et al. [26] demonstrate that specific molecules mediate the process of cell adhesion through either cell–matrix or cell–cell interactions that include integrins, cadherins, members of the immunoglobulin superfamily and selectins. The HeLa cell adhesion on antibody/metal/polysaccharide films has been studied by using EIS [27], in an additional confirmation that the impedance technique is a good tool for investigating cell adhesion on biopolymer surfaces.

Previous studies suggest that the non-specific cell-material adhesion seems to be due to the occurrence of weak chemical bonding (such as hydrogen bonding, electrostatic, polar or ionic interactions) between the various molecules on the cell membrane and the functional groups on the polymers. In addition, this type of interaction occurs due to the absence extracellular matrix proteins (EMP) or their functional parts [28–30]. The improvement of cell adhesion and growth on surfaces without EMP is obtained by coating of materials with different biological molecules that could provide the adhesive properties and the required environment for the cells' adherence and survival [31].

The Bode plots of the SCB and SCB–hWJMSC biosystems are presented in Fig. 6. As one can easily note, these two plots show differences in the magnitude of the impedance at high frequency ranges; namely, the impedance magnitude of hWJMSC at high frequency was higher than in the absence of hWJMSC. Also, while there is a clear distinction between the dielectric responses of the SCB films of different thickness, only small changes can be noticed in the impedance values at high frequencies (Fig. 6). The increase in the dielectric response for the SCB3 film (Fig. 6c) can be explained by the blockage to the displacement of ions that arises near of the surface [32].

The typical electrical interface associated to the use of SCB films as support to culture cells can be represented by the model electrical circuit shown in Fig. 7a. The proposed equivalent circuit includes not only the ohmic resistance of the electrolyte solution (R_Ω) and the Warburg impedance (W) that represents both the bulk properties of the electrolyte solution and the diffusion features of the redox probe in solution, but also the double-layer capacitance (C_{dl}) and the electron transfer resistance (R_{et}) related to the interfacial properties of the surface. Usually, R_{et} controls the interfacial electron-transfer rate between the solution and the electrode [33]. In addition, R_{et} is equal to the semicircle diameter at higher frequencies. The impedance data were fitted to a Randles equivalent circuit by use of a Boukamp non-linear least square fitting program [34] (Fig. 7a). Our results demonstrate that the changes in R_Ω and R_{et} were much larger than those for the other impedance parameters. Thus, R_{et} appears as a suitable signal for assessing the interfacial properties of the SCB during the cell adhesion procedure.

Table 1 shows the equivalent circuit parameters of the fitting curves (Fig. 7b) for the various steps of the monitoring of the hWJMSC adhesion. Generalized observations of EIS spectra during consecutive modification processes

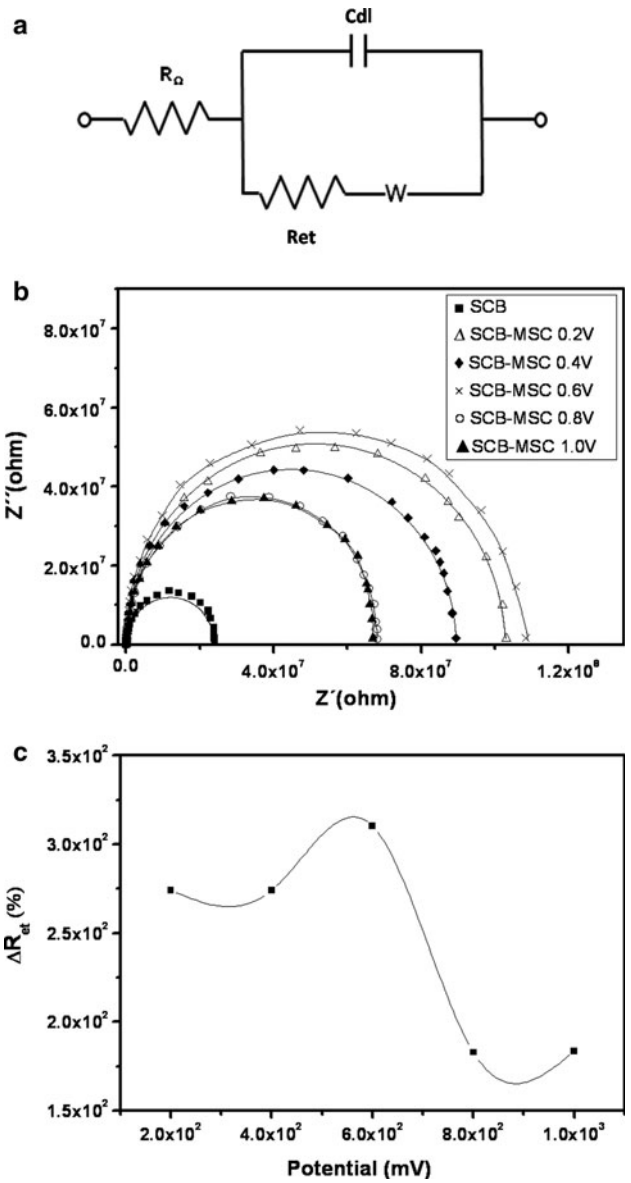

Fig. 7 Equivalent circuit (**a**) adopted to fit the impedance data and Nyquist plots (**b**) of the steps of cellular adhesion, before and after SCB exposition to hWJMSC: SCB (*filled square*), SCB–hWJMSC 0.2 V (*open triangle*), SCB–hWJMSC 0.4 V (*filled lezenge*), SCB–hWJMSC 0.6 V (*times*), SCB–hWJMSC 0.8 V (*open circle*) and SCB–hWJMSC 1.0 V (*filled triangle*). *Solid lines* correspond to the fitting using the obtained Randles parameters. ΔR_{et} % of SCB–hWJMSC adhesion process at different values of the applied potential (**c**)

of the biopolymer associated to the formation of SCB–hWJMSC systems show that, after the hWJMSC adhesion, the values of R_{et} of the equivalent circuit increase significantly, while the C_{dl} values are reduced. The EIS spectra showed the highest R_{et} at 0.6 V. This behavior illustrates that during the contact it was possible to establish specific interactions between the hWJMSC and the SCB surface, confirming the biocompatibility between them. As shown in Table 1, the resistance charge transfer magnitude was higher in the case when stem cells were present (~82.40 MΩ) than in the case of pure SCB films (~23.99 MΩ).

In Fig. 7b we show how the application of an external potential affects the electron-transfer resistance, both before and after cell adhesion to the SCB surface. The results presented in Fig. 7 clearly indicate that after the hWJMSC recognizes and adheres to the carbohydrates present in the SCB film, there is an increase in the value of the charge transfer (R_{et}).

The performance of the SCB as a matrix to cell adhesion was quantitatively evaluated by calculating the relative variation of the electron transfer resistance (ΔR_{et}), which is defined as

$$\Delta R_{et}\ \% = \left(\frac{R_{(SCB-HWJMSC)} - R_{SCB}}{R_{SCB}}\right) \times 100, \qquad (1)$$

where R_{SCB} is the value of the electron-transfer resistance of the pure SCB film, and $R_{(SCB-hWJMSC)}$ is the value of the electron-transfer resistance of the SCB modified after exposition to MSC. The change ΔR_{et} in the electron transfer resistance was determined for different values of the applied potential (Fig. 7c). During the interaction of the SCB film with stem cells, the EIS curves displayed an increasing impedance response when compared to the unmodified SCB film. Since the values of ΔR_{et} correlate well with the number of cells specifically bound to the SCB surface, this parameter can be used to assess the biocompatibility of the sugar cane biopolymer. The results indicate that ΔR_{et} is influenced by the value of the applied potential, with an obvious maximum observed for 0.6 V both in the pure SCB and SCB–hWJMSC systems. In this case, the ΔR_{et} value is related to the more stable stem cell adhesion on the SCB film. Therefore, the results we have obtained demonstrate that the electric impedance technique could be used for the sensitive monitoring of the dynamic of the SCB–hWJMSC interaction.

Cell adhesion is an important analysis by which implant surfaces may be evaluated to determine suitability for medical use. Thus, a stable connection between the biomaterial surface and the surrounding tissue is one of the most important prerequisites for the long-term [35] success of implants. In addition, some elements of the extracellular matrix are synthesized and secreted by cells in culture, where they may play a role in cell-substratum and cell–cell adhesion. One protein that is of particular interest in determining the relationship between cells and their substrate is fibronectin, as it represents one of the major molecules mediating cell attachment and playing critical roles in cell survival, proliferation and differentiation [36]. Then, the biocompatibility of SCB films in allowing MSC growth was studied since the osteoblastic cells adhesion is of interest for applications in tissue engineering [37].

Table 1 Values of the equivalent circuit elements from fitted impedance result

Sample	Potential (V)	R_Ω (Ω)	C_{dl} (F)	R_{et} (MΩ)	W
Metal electrode	–	1.01×10^{6}	2.41×10^{-12}	7.85	4.93×10^{10}
BPCA	0.2	2.50×10^{4}	2.26×10^{-2}	24.00	2.61×10^{1}
BPCA-MSC	0.2	9.10×10^{3}	2.30×10^{-11}	89.43	3.95×10^{10}
BPCA-MSC	0.4	9.10×10^{3}	2.30×10^{-11}	89.43	3.95×10^{10}
BPCA-MSC	0.6	8.80×10^{3}	2.24×10^{-11}	98.08	4.12×10^{10}
BPCA-MSC	0.8	1.49×10^{4}	2.23×10^{-11}	67.68	4.27×10^{10}
BPCA-MSC	1.0	1.51×10^{4}	2.22×10^{-11}	67.76	4.71×10^{10}

All measurements were performed in triplicate using the MSC adhered on SCB (three samples of each analysis) and system control (SCB1-3), obtaining $n = 9$ for each analyzed sample

4 Conclusions

The adhesion of MSC was tested on a biopolymer film as a manner to evaluate the ability of SCB films as cell culture substrates. This study is the first description of impedimetric analysis of the use of SCB films as a matrix model system for MSC from hWJMSC adhesion. The MSC reacted independently of the thickness to the SCB film. We have demonstrated that SCB can be used as a good platform for the cell adhesion. Our results suggest that EIS technique is an useful technique for evaluating the MSC from hWJMSC adhesion on SCB films.

Acknowledgments We dedicated this work to Prof. Oleg V. Krasilnikov (*in memoriam*). Fragoso would like to thank FACEPE for a graduate scholarship. Andrade and Oliveira are also gratefully for CNPq financial support (Grant 310305/2012-8 and 310361/2012-5, respectively). We thank the Hospital de Ávila (Recife, PE) for providing human umbilical cord samples.

References

1. Guimard NK, Gomez N, Schimidt CE. Conducting polymers in biomedical engineering. Prog Polym Sci. 2007;32:876–921.
2. Sengupta D, Heilshorn SC. Protein-engineered biomaterials: highly tunable tissue engineering scaffolds. Tissue Eng Part B. 2010;16:285–93.
3. Coelho MC, Carrazoni PG, Monteiro VL, Melo FA, Mota RA, Tenório F. Biopolímero produzido a partir da cana-de-açúcar para cicatrização cutânea. Acta Cir Bras. 2002;17:11–3.
4. Albuquerque PCUC, Santos SM, Aguiar JLA, Filho NP, de Mello RJV, Costa MLCR, Olbertz CMCA, Almeida TMS, Da Silva Santos AH, da Silva JC. Comparative macroscopic study of osteochondral defects produced in femurs of rabbits repaired with biopolymer gel cane sugar. Rev Bras Ortop. 2011;46:577–84.
5. Carvalho Junior AM, Santos MM, Barkokébas BB, Aguiar JLA, Lima SVC, Dambros M. Characterization of the deposition of collagen fibers and lithogenic potential in bladder of rats submitted to a sugar cane biopolymer graft. Int Braz J Urol. 2012;38:544–51.
6. Aguiar J, Lins E, Marques S, Coelho A, Rossiter R, Melo R. Sugarcane biopolymer patch in femoral artery angioplasty in dogs. Acta Cir Bras. 2007;22:77–81.
7. Baksh D, Song L, Tuan SR. Adult mesenchymal stem cells: characterization, differentiation, and application in cell and gene therapy. J Cell Mol Med. 2004;8:301–16.
8. Chen FH, Rousche KT, Tuan RS. Technology insight: adult stem cells in cartilage regeneration and tissue engineering. Nat Clin Pract Rheumatol. 2006;2:373–82.
9. Chamberlain JR, Schwarze U, Wang PR, Hirata RK, Hankenson KD, Pace JM, Underwood RA, Song KM, Sussman M, Byers PH, Russell DW. Gene targeting in stem cells from individuals with osteogenesis imperfect. Science. 2004;303:1198–201.
10. Grinnemo KH, Månsson A, Dellgren G, Klingberg D, Wardell E, Drvota V, Tammik C, Holgersson J, Ringdén O, Sylvén C, Le Blanc K. Xenoreactivity and engraftment of human mesenchymal stem cells transplanted into infarcted rat myocardium. J Thorac Cardiovasc Surg. 2004;127:1293–300.
11. Muzzarelli RAA. Chitosan composites with inorganics, morphogenetic proteins and stem cells, for bone regeneration. Carbohyd Polym. 2011;83:1433–45.
12. Houa Y, Helali S, Zhang A, Jaffrezic-Renault N, Martlet J, Minic C, Gorojankina T, Persuy MA, Pajot-Angy E, Salesse R, Bessueille F, Samitier J, Enachid A, Akimov V, Reggiani L, Pennetta C, Alfinito E. Immobilization of rhodopsin on a self-assembled multilayer and its specific detection by electrochemical impedance spectroscopy. Biosens Bioelectron. 2006;21:1393–402.
13. Navrátilová I, Skládal P. The immunosensors for measurement of 2,4-dichlorophenoxyacetic acid based on electrochemical impedance spectroscopy. Bioelectrochemistry. 2004;62:11–8.
14. Schwan HP. Mechanisms responsible for electrical properties of tissues and cell suspensions. Med Prog Technol. 1993;19:163–5.
15. Malmivuo J, Plonsey R. Bioelectromagnetism: principles and applications of bioelectric and biomagnetic fields. New York: Oxford University Press; 1995.
16. Reininger-Mack A, Thielecke H, Robitzki AA. 3D-biohybrid systems: applications in drug screening. Trends Biotechnol. 2002;20:56–61.
17. Castro JEC, Pólo JL, Labrado GRH, Cañete VP, Rama CG. Bioelectrochemical control of neural cell development on conducting polymers. Biomaterials. 2010;31:9244–55.
18. Xue Y, Bao L, Xiao X, Ding L, Lei J, Ju H. Noncovalent functionalization of carbon nanotubes with lectin for label-free dynamic monitoring of cell-surface glycan expression. Anal Biochem. 2011;410:92–7. doi:10.1016/j.ab.2010.11.019.
19. Luna DMN, Falcao EPS, Melo SJ, Andrade CAS. Interfacial properties of a novel pyrimidine derivative and poly(ethylene glycol)-grafted phospholipid floating monolayers. Coll Surf A. 2011;373:22–8.

20. Silverstein RM, Webster FX, Kiemle DJ. Identificação espectrofotométrica de compostos orgânicos. 7th ed. Rio de Janeiro: LTC; 2006.
21. Lanza RP, Langer RS, Vacanti J. Principles of tissue engineering. 3rd ed. Amsterdam: Elsevier; 2007.
22. Sarró E, Lecina M, Fontova A, Solá C, Gódia F, Cairó JJ, Bragós R. Electrical impedance spectroscopy measurements using a four-electrode configuration improve on-line monitoring of cell concentration in adherent animal cell cultures. Biosens Bioelectron. 2012;31:257–63.
23. Trinkaus JP. Cells into organs. New Jersey: Prentice-Hall; 1969.
24. Sharon N, Ofek I. Fighting infectious diseases with inhibitors of microbial adhesion to host tissues. Crit Rev Food Sci Nutr. 2002;42:267–72.
25. Chung TW, Limpanichpakdee T, Yang MH, Tyan YC. An electrode of quartz crystal microbalance decorated with CNT/chitosan/fibronectin for investigating early adhesion and deforming morphology of rat mesenchymal stem cells. Carbohyd Polym. 2011;85:726–32.
26. Guo M, Chen K, Nie L, Yao S. Monitoring of cell growth and assessment of cytotoxicity using electrochemical impedance spectroscopy. Biochim Biophys Acta. 2006;1760:432–9.
27. Jiang X, Tan L, Zhang B, Zhang Y, Tang H, Xie Q, Yao S. Detection of adherent cells using electrochemical impedance spectroscopy based on molecular recognition of integrin b1. Sens Act B. 2010;149:87–93.
28. Bacakova L, Mares V, Bottone MR, Pellicciari C, Lisa V, Svorcik V. Fluorine ion-implanted polystyrene improves growth and viability of vascular smooth muscle cells in culture. J Biomed Mater Res. 2000;49:369–79.
29. Bacakova L, Mares V, Lisa V, Svorcik V. Molecular mechanisms of improved adhesion and growth of an endothelial cell line cultured on polystyrene implanted with fluorine ions. Biomaterials. 2000;21:1173–9.
30. Bacakova L, Filova E, Rypacek F, Svorcik V, Stary V. Cell adhesion on artificial materials for tissue engineering. Physiol Res. 2004;53:35–45.
31. Sachlos E, Czernuszka JT. Making tissue engineering scaffolds work. Review: the application of solid freeform fabrication technology to the production of tissue engineering scaffolds. Eur Cell Mater. 2003;5:29–39 discussion 39-40.
32. Gheorghe M, Guiseppi-Elie A. Electrical frequency dependent characterization of DNA hybridization. Biosens Bioelectron. 2003;19:95–102.
33. Randles JEB. Kinetics of rapid electrode reactions. Discuss Faraday Soc. 1947;1:11–9.
34. Boukamp BA. A package for impedance/admittance data analysis. Solid State Ionics. 1986;18–19:136–40.
35. Demetrescu I, Pirvu C, Mitran V. Effect of nano-topographical features of Ti/TiO_2 electrode surface on cell response and electrochemical stability in artificial saliva. Bioelectrochemistry. 2010;79:122–9.
36. Yamada KM. Fibronectin domains and receptors. In: Mosher DE, editor. Fibronectin. San Diego: Academic Press, Inc.; 1989.
37. Anselme K. Osteoblast adhesion on biomaterials. Biomaterials. 2000;21:667–81.